applied sciences

MDPI

Article

RNA–CTMA Dielectrics in Organic Field Effect Transistor Memory

Lijuan Liang [1,*], Yabo Fu [1], Lianfang Li [1], Huan Zheng [1], Xianfu Wei [1], Yen Wei [2] and Norihisa Kobayashi [1,3]

1 Beijing Institute of Graphic Communication, Beijing 102600, China; fuyabo@126.com (Y.F.); 195280893@qq.com (L.L.); yuzhouhero@126.com (H.Z.); weixianfu@bigc.edu.cn (X.W.); koban@faculty.chiba-u.jp (N.K.)
2 Department of Chemistry, Tsinghua University, Beijing 100084, China; weiyen@tsinghua.edu.cn
3 Department of image & Materials science, Graduate School of Advanced Integration Science, Chiba University, 1-33 Yayoi-cho, Inage-ku, Chiba 263-8522, Japan
* Correspondence: lianglijuan@bigc.edu.cn

Received: 23 April 2018; Accepted: 18 May 2018; Published: 29 May 2018

Abstract: In recent years, biopolymers are highly desired for their application in optic electronic devices, because of their unique structure and fantastic characteristics. In this work, a non-volatile memory (NVM) device based on the bio thin-film transistor (TFT) was fabricated through applying a new RNA–CTMA (cetyltrimethylammonium) complex as a gate dielectric. The physicochemical performance, including UV, CD spectral, thermal stability, surface roughness, and microstructure, has been investigated systematically. The RNA–CTMA complex film exhibits strong absorption with a well-defined absorption peak around 260 nm, the RMS roughness is ~2.1 nm, and displayed excellent thermal stability, up to 240 °C. In addition, the RNA–CTMA complex-based memory device shows good electric performance, with a large memory window up to 52 V. This demonstrates that the RNA–CTMA complex is a promising candidate for low cost, low-temperature processes, and as an environmentally friendly electronic device.

Keywords: RNA-CTMA; OTFT; transistor memory

1. Introduction

In recent years, biopolymers as environmental friendly materials have attracted much attention, due to their potential applications as novel optical and electronic components. For example, organic thin-film transistors (OTFTs) have been prepared with biopolymers because these devices can be fabricated with large-scale manufacturing techniques, such as screen printing, spin-coating, gravure printing, and others. Also, as biopolymers are contained in abundant resources, the fabricated devices are generally of low-cost [1–5]. These fascinating characteristics of OTFTs make them potential candidates for moveable memory devices [6], active matrix displays [7], radio frequency identification tags [8], and biochemical sensors [9].

The selection of biopolymer is essential to fabricate a BioTFT memory device with good performance, as various biopolymer dielectrics have significant effects on the electric properties of OTFT memory devices [10]. Okahata et al. have first reported the preparation of DNA–cetyltrimethylammonium (CTMA) complexes, which were soluble in organic solvents, and proven to effectively reduce counter sodium ions [11]. After that, many researchers utilized various cationic surfactants to prepare electronic devices, including OTFTs, organic light emitting diodes (OLEDs), and even solar cells [12–18]. In our previous work [19–21], we have improved the performance of BioTFT memory devices through applying biopolymer

DNA–octadecyltrimethylammonium (OTMA), and DNA–lauroylcholine (Lau) complex as the gate dielectric. The ON/OFF current ratio of DNA–OTMA-based BiOTFT devices has been improved significantly. The device exhibited a large memory window during recording of the transfer characteristic, and also, a stable memory performance based on switching response.

Ribonucleic acid (RNA), one of the famous biopolymers, is a ribonucleic acid containing genetic instruction on the sequence of the hydroxyl groups, which could be applied as a good alternative to DNA. Purified RNA could be soluble in polar solvents such as water, and the resulting films are also water-sensitive, and have insufficient mechanical strength for applications in the photonics and optoelectronics fields [22,23]. So, there are still many works need to be done on the modification of RNA-based complex to improve the electric performance.

In this work, we utilized RNA–CTMA complex to fabricate the BioTFT memory device. The RNA–CTMA complex film was obtained via an ion exchange reaction, and the structure evolution of the film has been studied by the optical analysis, including UV spectra and circular dichroism (CD) spectra. Furthermore, the thermal stability, surface roughness, and microstructure of the RNA complex have been investigated. Finally, the OTFT devices were fabricated and characterized, which exhibit a large memory window and stable device performance.

2. Experimental

Materials and film preparations. The sodium salts of RNA were purchased from Sigma-Aldrich, St. Louis, USA. Pentacene (98% purity) was supplied by Naad Co., Ltd, Tokyo, Japan. Butanol, CTMA (98% purity), and common chemicals were purchased from Tokyo Chemical Industry Co., Ltd., Tokyo, Japan. The RNA–CTMA complex film was prepared by spin-coating it onto an indium tin oxide (ITO) glass substrate, and the film thickness of the RNA–CTMA surfactant complex films were about 1 μm.

Device fabrications. BioTFT memory devices were fabricated according to the former study [19]. The BioTFT structure using a top contact and gate bottom geometry is schematically depicted in Figure 1.

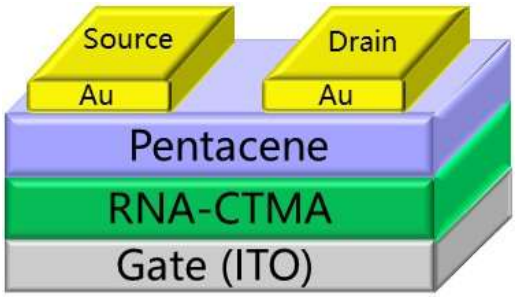

Figure 1. Schematic representations of the BioTFT memory using RNA–CTMA (cetyltrimethylammonium) as the gate dielectric layer.

Film and device characterizations. UV–vis absorption spectral of the samples were measured using a spectrophotometer (JASCO, V-570). Circular dichroism (CD) spectral of the RNA–CTMA film was measured using a CD spectrometer (JASCO, J-820). Film morphology was performed using AFM scanning probe microscope (Seiko, SPA-400) and X-ray diffraction (D/MAX2000/PC, Rigaku Corporation, Japan). Thermal properties of RNA–CTMA were analyzed by the DSC analyzer, (Bruker, DE, 3200 SA). All electric measurements were carried out using a Keithley 4200 semiconductor parameter analyzer under dark conditions in vacuo under the non-clean room, ambient-air environment. The surface roughness of the RNA–CTMA complex and pentacene film was recorded with a Dektak surface profilometer.

3. Results and Discussion

The optical absorption properties of RNA–CTMA complex thin-film are shown in Figure 2a. A broad absorption peak was obtained at 260 nm, which could be assigned to the signature of π–π* transition of the nuclei bases. The same peak has also been observed in the DNA–OTMA complex as previously reported [19]. Above 300 nm, there is no observable absorption in the RNA–CTMA film, which exhibits excellent optical transparency in the visible range, and indicates RNA–CTMA was also the potential candidate in the application of transparent electronic devices.

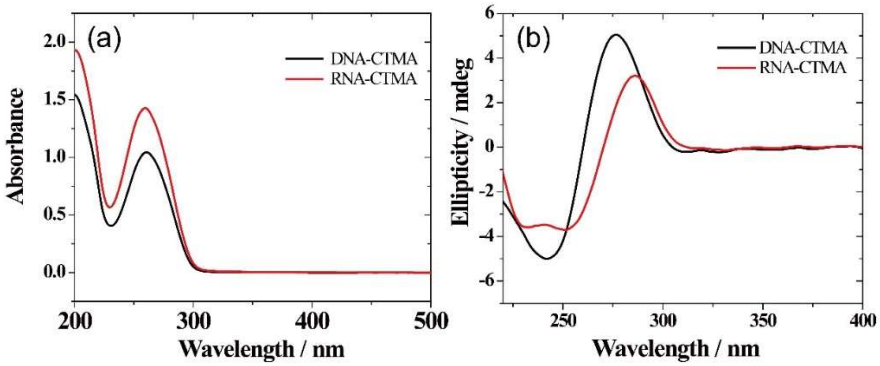

Figure 2. (**a**) UV spectra of the RNA–CTMA complex. (**b**) CD spectra of the RNA–CTMA complex.

In order to further study the configuration of the RNA–CTMA complex, the CD spectrum of the RNA–CTMA complex was measured, which is an important toll to investigate the characteristics of the secondary structure of biopolymer [24]. As shown in the Figure 2b, two negative Cotton effects at about 251 nm and 232 nm, and a positive Cotton effect at about 286 nm, were observed, which are different from the natural DNA and DNA–CTMA complex, as shown in previous studies [19]. Compared with DNA–CTMA complex, the Cotton effect in the RNA–CTMA complex is weaker, indicating that the RNA–CTMA complex shows weaker structure regularity than that in DNA–CTMA complex. The reason could be attributed to the single helix structure of the RNA complex.

The IR spectra of the RNA and RNA–CTMA film were measured and compared, as shown in Figure 3. The different wave numbers of each different film are summarized in Table 1. As shown in the table, compared with the RNA film, the vibration wave number of antisymmetric and symmetric of PO_2 group in RNA–CTMA film showed a red shift, which was attributed to the interaction between RNA and the CTMA surfactant, indicating that the CTMA group was successful aligned to RNA molecules.

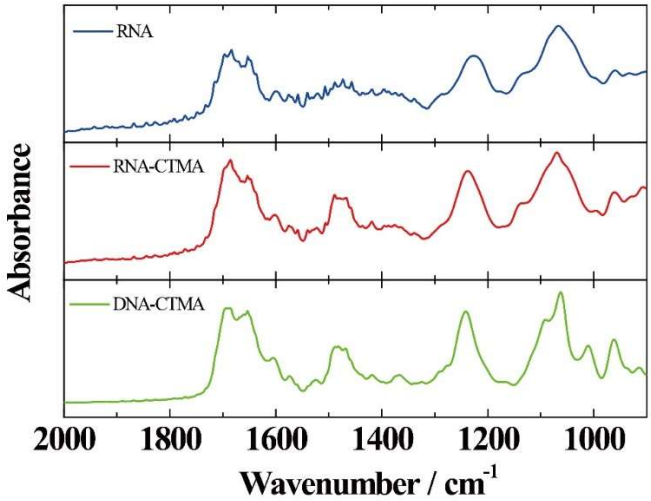

Figure 3. IR spectra of (**top**) RNA, (**middle**) RNA–CTMA, and **(bottom**) DNA–CTMA films.

Table 1. Wavenumber of RNA, RNA–CTMA, and DNA–CTMA film.

RNA	RNA–CTMA	DNA–CTMA	Assignments
1226	1237	1240	PO_2 antisymmetric
1127	1134	1089	PO_2 symmetric
1066	1069	1062	C–O sugar
1000	996	1010	Sugar ring

Furthermore, thermostability of RNA–CTMA was also measured as one of the important parameters of physical and chemical performance. The upper limit of the temperature where they can retain the key properties defines their processing temperature and device working temperatures. Hence, the thermogravimetry analysis (TGA) in nitrogen atmosphere has been used to investigate the polymers. Figure 4a shows the thermal degradation curves for CTMA alone, and RNA–CTMA surfactant complex, respectively. Both the samples exhibit good thermal stability and, especially, it is very surprising to find that the CTMA cationic surfactant can be stable until 250 °C. In addition, the RNA–CTMA surfactant complex also shows excellent heat resistance, and is thermally stable up to 240 °C. As a consequence, the RNA complex can tolerate normal printing and processing, and the devices could work in traditional circuits. Especially, the RNA complex may also be a potential candidate for a temperature sensor that operates under high temperature environments.

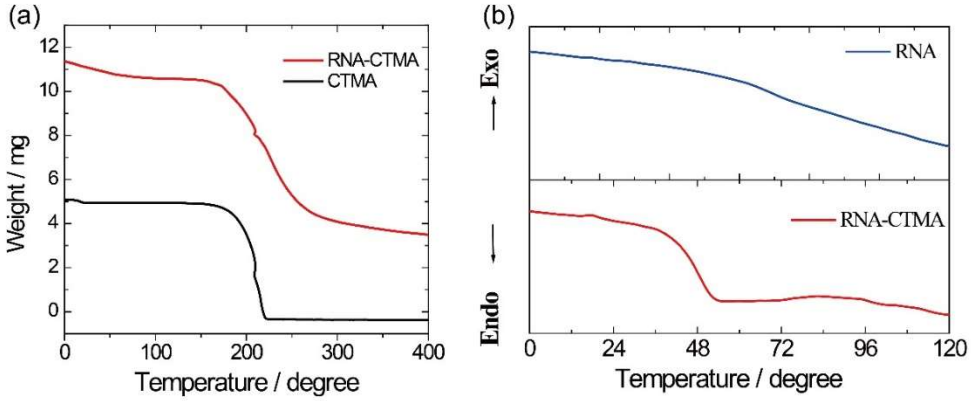

Figure 4. (**a**) Thermogravimetric (TG) curves of CTMA and RNA–CTMA. (**b**) The DSC curve of the RNA and RNA–CTMA complex.

Figure 4b shows the DSC curve of the RNA and RNA–CTMA complex film at a temperature range from 0 to 120 °C, with a heating rate of 10 °C/min. A baseline shift at around 55 °C and 42 °C of RNA and RNA–CTMA complex were obtained, respectively, which could be attributed to the phase transition. These results indicate that as the temperature increases and exceeds the phase transition, the volume of the RNA and RNA–CTMA complex would be expected, and the singe helix main chain could be moved, so the dipoles aligning to the main chain also could be oriented along the direction of the applied voltage.

Besides the optical, structural, and thermal properties of the complex, the morphology of the complex film was also characterized. For electronic devices, the surface roughness of the biopolymer film plays an important role, especially when it acts as the interface for charge accumulation and transport [25]. For example, in the BioTFT memory device, the holes transport at the interface between RNA–CTMA film and organic semiconductor film, and thus, defects or surface fluctuations could deteriorate the transport properties. In order to study the film morphology and microscopic structure of the RNA–CTMA film, atomic force micrographs (AFM) and X-ray diffraction patterns were investigated, respectively. Figure 5a exhibits the atomic force microscopy (AFM) image of the RNA–CTMA film depositing on the ITO substrates. The root mean square (rms) surface roughness

of RNA–CTMA film (thickness of 1 μm) is ~2.1 nm, which is quite smooth for such a thick film, and allows it to be a functional interface for charge transport in TFTs. Figure 5b shows the result of the X-ray diffraction patterns of RNA–CTMA complex. A sharp diffraction peak was observed in the small-angle region, corresponding to a spacing of about 39 Å in the RNA–CTMA complex film. This sharp peak corresponds to the diameter of the packed RNA complex structure, indicating an ordered structure of the film, and may help reduce gate leakage during device operations.

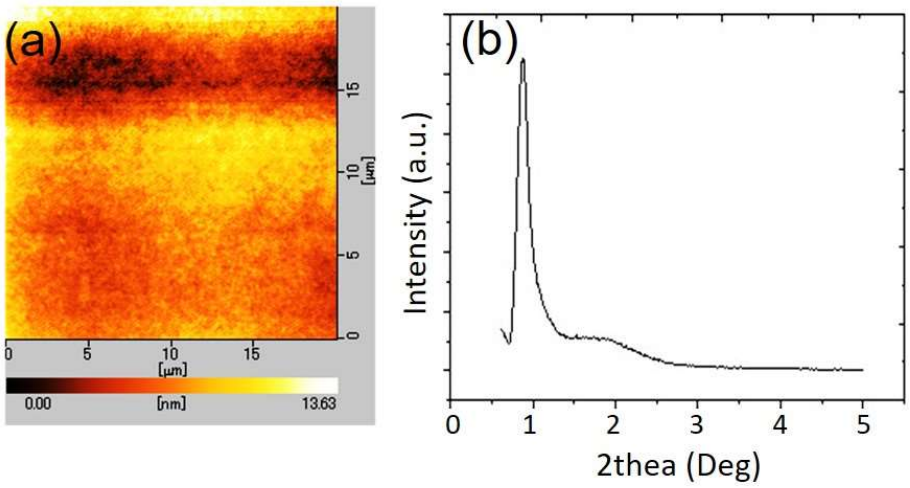

Figure 5. (**a**) Topological graph of the RNA–CTMA complex film obtained by atomic force microscopy (AFM). The root mean square (rms) surface roughness is measured to be 2.1 nm. (**b**) X-ray diffraction patterns of the RNA–CTMA complex.

The BioTFT memory device was fabricated using the RNA–CTMA as the gate dielectric, and the measured transfer characteristics (I_{DS}–V_G) are shown in Figure 6. The dielectric DNA–CTMA polymer applied as control experiments, herein, have also been carried out. Typical memory windows were observed, and indicated that the RNA–CTMA complex film could work as the gate dielectric layer to prepare the memory device. The OFF currents were 3.5×10^{-10} A and 9.7×10^{-11} A for the devices with RNA–CTMA and DNA–CTMA complexes, respectively, indicating that the resistivity of both the biopolymer films could satisfy the operating requirement. The field effect mobility was calculated by fitting the plot of the square root of I_{DS} versus V_G, using the following equation:

$$I_{DS} = \frac{W}{2L} C \mu_{sat} (V_G - V_{th})^2. \quad (1)$$

Here, I_{DS} is the saturation drain current, V_G is the gate voltage, V_{th} is the threshold voltage, C is the capacitance of gate dielectric per unit area, and W and L are the width and length of the channel of the device, respectively. The field-effect mobility of the RNA–CTMA-based device was calculated to be 0.108 $cm^2/V{\cdot}s$. In addition, from the transfer characteristic, the device based on RNA–CTMA has a threshold voltage V_{th} of −34.5 V. The memory window is 52 V, which could be caused by the dipoles in the RNA–CTMA complex film [20]. The values are comparable with the values reported in recent years, indicating that the RNA–CTMA may be a potential candidate for the dielectric material for non-volatile memory device.

Note that the ON current of the DNA–CTMA-based device was higher than that of the RNA–CTMA-based device. This result may be related to the morphological difference of the pentacene layer deposited on these different films. The AFM of the semiconducting pentacene film (thickness of 50 nm) was investigated as shown in Figure 7, comparing the films deposited on top of the RNA–CTMA and DNA–CTMA complex film, respectively. The pentacene film deposited on either complex film shows a highly crystalline structure. The average crystal grain size depositing on DNA–CTMA is

calculated to be about 167 nm, whereas the value for the crystals grown on RNA–CTMA complex film is about 125 nm. In addition, the crystal depositing on RNA–CTMA film exhibits a few voids, which could be due to the slightly lower surface free energy on the RNA–CTMA film that could easily induces clusters during crystal deposition. Thus, the smaller average grain size together with some voids on the RNA–CTMA film are probably suppressing the carrier transport along the electric field, and thus, a slightly lower current level in the OTFTs.

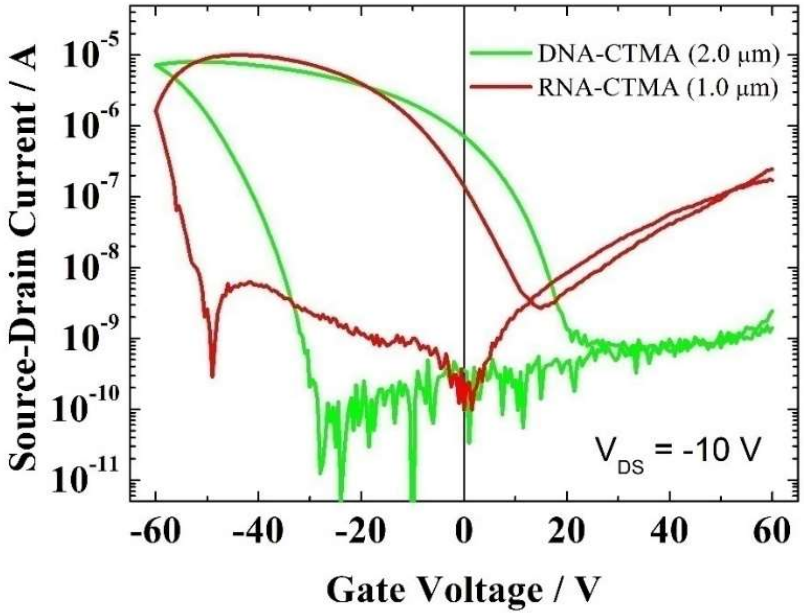

Figure 6. Transfer characteristics of BiOTFTs with DNA and RNA complex as the gate dielectric.

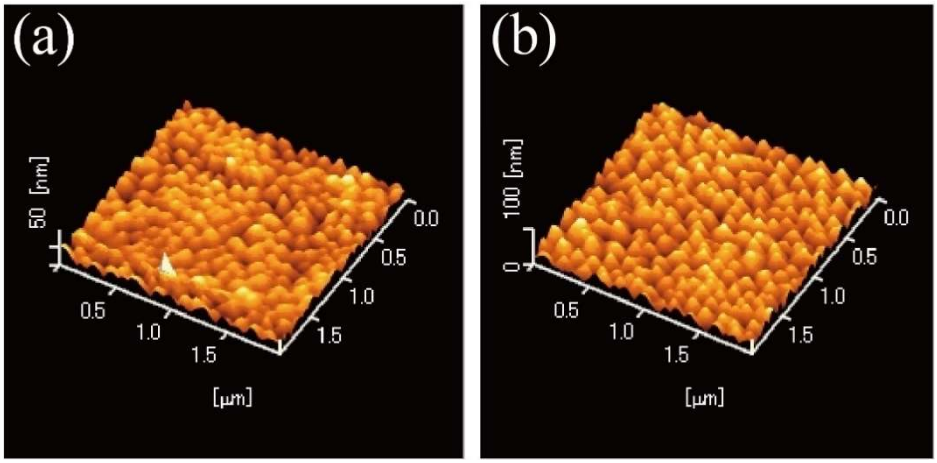

Figure 7. AFM topographical images of pentacene deposited on (**a**) RNA–CTMA and (**b**) DNA–CTMA film.

4. Conclusions

In summary, a non-volatile transistor memory device was fabricated based on RNA–CTMA as the gate dielectric, which has been demonstrated for the first time. The memory device exhibited good electronic performance with a large memory window, which could be caused by the dipoles that existed in the RNA complex. From the results of DSC, AFM, and XRD, we found that the RNA–CTMA complex film exhibited a baseline at around 42 °C, small roughness of 2.1 nm, and ordered crystal structure.

Therefore, the RNA–CTMA complex that comes from torula can be a promising candidate for the preparation of low-cost, low-temperature processing, and environmentally friendly electronic devices.

Author Contributions: L.L. designed and carried out the experiment. Y.F., L.L. and H.Z. processed the test data. With the help of Y.W. and K.N., L.L. wrote and completed the paper. All authors read and approved the final manuscript.

Funding: This study was funded by the National Natural Science Foundation of China (21604005), the China postdoctal science foundation (2015M581007, 2016T90047), the general project of science and technology of Beijing Municipal Education Commission (SQKM201610015006), and the National Key R&D Program (2016YFC0204202).

Conflicts of Interest: The authors declare no conflict of interest.

References

1. Magliulo, M.; Manoli, K.; Macchia, E.; Palazzo, G.; Torsi, L. Tailoring Functional Interlayers in Organic Field-Effect Transistor Biosensors. *Adv. Mater.* **2015**, *27*, 7528–7551. [CrossRef] [PubMed]
2. Chang, J.W.; Wang, C.G.; Huang, C.Y.; Tsai, T.D.; Guo, T.F.; Wen, T.C. Chicken Albumen Dielectrics in Organic Field-Effect Transistors. *Adv. Mater.* **2011**, *23*, 4077–4081. [CrossRef] [PubMed]
3. Kim, S.J.; Jeon, D.B.; Park, J.H.; Ryu, M.K.; Yang, J.H.; Hwang, C.S.; Kim, G.H.; Yoon, S.M. Nonvolatile memory thin-film transistors using biodegradable chicken albumen gate insulator and oxide semiconductor channel on eco-friendly paper substrate. *ACS Appl. Mater. Interfaces* **2015**, *7*, 4869–4874. [CrossRef] [PubMed]
4. Kim, Y.S.; Jung, K.H.; Lee, U.R.; Kim, K.H.; Hoang, M.H.; Jin, J.-I.; Choi, D.H. High-performance, low-operating voltage, and solution-processable organic field-effect transistor with silk fibroin as the gate dielectric. *App. Phys. Lett.* **2014**, *96*. [CrossRef]
5. Stadler, P.; Oppelt, K.; Singh, T.B.; Grote, J.G.; Schwödiauer, R.; Bauer, S.; Brezina, H.P.; Bäuerle, D.; Sariciftci, N.S. Organic field-effect transistors and memory elements using deoxyribonucleic acid (DNA) gate dielectric. *Org. Electron.* **2007**, *8*, 648. [CrossRef]
6. Jeng, H.Y.; Yang, T.C.; Yang, L.; Grote, J.G.; Chen, H.L.; Hung, Y.C. Non-volatile resistive memory device based on solution-processed natural DNA biomaterial. *Org. Electron.* **2017**, *54*, 216–221. [CrossRef]
7. Zhou, L.; Wanga, A.; Wu, S.C.; Sun, J.; Park, S.; Jackson, T.N. All-organic active matrix flexible display. *Appl. Phys. Lett.* **2006**, *88*, 083502. [CrossRef]
8. Baude, P.F.; Ender, D.A.; Haase, M.A.; Kelley, T.W.; Muyres, D.V.; Theiss, S.D. Pentacene-based radio-frequency identification circuitry. *Appl. Phys. Lett.* **2003**, *82*, 3964–3966. [CrossRef]
9. Parashkov, R.; Becker, E.; Ginev, G.; Riedl, T.; Brandes, M.; Johannes, H.H.; Kowalsky, W. Organic vertical-channel transistors structured using excimer laser. *Appl. Phys. Lett.* **2004**, *85*, 5751–5753. [CrossRef]
10. Naber, R.C.G.; Asadi, K.; Blom, P.W.M.; Leeuw, D.M.D.; Boer, B.D. Organic Nonvolatile Memory Devices Based on Ferroelectricity. *Adv. Mater.* **2010**, *22*, 933–945. [CrossRef] [PubMed]
11. Tanaka, K.; Okahata, Y. A DNA−Lipid Complex in Organic Media and Formation of an Aligned Cast Film1. *J. Am. Chem. Soc.* **1996**, *118*, 10679. [CrossRef]
12. Zalar, P.; Kamkar, D.; Naik, R.; Ouchen, F.; Grote, J.G.; Bazan, G.C.; Nguyen, T.-Q. DNA electron injection interlayers for polymer light-emitting diodes. *J. Am. Chem. Soc.* **2011**, *133*, 11010. [CrossRef] [PubMed]
13. Grykien, R.; Luszczynska, B.; Glowacki, I.; Ulanski, J.; Kajzar, F.; Zgarian, R.; Rau, I. A significant improvement of luminance vs current density efficiency of a BioLED. *Opt. Mater.* **2014**, *36*, 1027. [CrossRef]
14. Gomez, E.F.; Venkatraman, V.; Grote, J.G.; Steckl, A.J. Exploring the Potential of Nucleic Acid Bases in Organic Light Emitting Diodes. *Adv. Mater.* **2015**, *27*, 7552. [CrossRef] [PubMed]
15. Gomez, E.F.; Venkatraman, V.; Grote, J.G.; Steckl, A. DNA Bases Thymine and Adenine in Bio-Organic Light Emitting Diodes. *Sci. Rep.* **2014**, *4*, 7105. [CrossRef] [PubMed]
16. Yusoff, A.; bin Mohd, R.; Kim, J.; Jang, J.; Nazeeruddin, M.K. New Horizons for Perovskite Solar Cells Employing DNA-CTMA as the Hole-Transporting Material. *ChemSusChem* **2016**, *9*, 1736–1742. [CrossRef] [PubMed]
17. Kumar, A.; Shukla, R.D.; Yadav, D.; Gupta, L.P. Friedel–Crafts alkylation of indoles in deep eutectic solvent. *RSC Adv.* **2015**, *5*, 52062–52065. [CrossRef]
18. Ensslen, P.; Gärtner, S.; Glaser, K.; Colsmann, A.; Wagenknecht, H.-A. A DNA–Fullerene Conjugate as a Template for Supramolecular Chromophore Assemblies: Towards DNA-Based Solar Cells. *Angew. Chem. Int. Ed.* **2016**, *55*, 1904–1908. [CrossRef] [PubMed]

19. Liang, L.; Yukimoto, T.; Uemura, S.; Kamata, T.; Nakamura, K.; Kobayashi, N. Structure of DNA-Octadecyltrimethylammonium Chloride Biopolymer Complex and the Application to Non-Volatile BiOTFT Memory. *Sci. Adv. Mater.* **2014**, *6*, 1516–1519. [CrossRef]
20. Liang, L.; Mitsumura, Y.; Nakamura, K.; Uemura, S.; Kamata, T.; Kobayashi, N. Temperature dependence of transfer characteristics of OTFT memory based on DNA-CTMA gate dielectric. *Org. Electron.* **2016**, *28*, 294–298. [CrossRef]
21. Yukimoto, T.; Uemura, S.; Kamata, T.; Nakamura, K.; Kobayashi, N. Non-volatile transistor memory fabricated using DNA and eliminating influence of mobile ions on electric properties. *J. Mater. Chem. C* **2011**, *21*, 15575. [CrossRef]
22. Grote, J.G.; Hopkins, F.K. Bio-organic semiconductor-field-effect-transistor based on deoxyribonucleic acid gate dielectric. *Appl. Phys.* **2006**, *100*, 024514.
23. Kwon, Y.W.; Lee, C.H.; Choi, D.H.; Jin, J.I. Materials science of DNA. *J. Mater. Chem.* **2009**, *19*, 1353–1380. [CrossRef]
24. Steckl, A.J.; Spaeth, H.; You, H.; Gomez, E.; Grote, J. DNA as an optical material. *Opt. Photonics News* **2011**, *22*, 34–39. [CrossRef]
25. Deman, A.L.; Erouel, M.; Lallemand, D.; Goutorbe, M.P.; Lang, P.; Tardy, J. Growth related properties of pentacene thin film transistors with different gate dielectrics. *J. Non-Cryst. Solids* **2008**, *354*, 1598–1607. [CrossRef]